applied sciences

MDPI

Article

Prediction of Ultimate Strain and Strength of FRP-Confined Concrete Cylinders Using Soft Computing Methods

Iman Mansouri [1], Ozgur Kisi [2], Pedram Sadeghian [3], Chang-Hwan Lee [4] and Jong Wan Hu [5,6,*]

1 Department of Civil Engineering, Birjand University of Technology, Birjand 97175-569, Iran; mansouri@birjandut.ac.ir
2 School of Natural Sciences and Engineering, Ilia State University, Tbilisi 0162, Georgia; ozgur.kisi@iliauni.edu.ge
3 Department of Civil and Resource Engineering, Dalhousie University, 1360 Barrington Street, Halifax, NS B3H 4R2, Canada; Pedram.Sadeghian@dal.ca
4 Research Institute of Structural Engineering & System, DongYang Structural Engineers Co., Ltd., Seoul 05836, Korea; chlee@dysec.co.kr
5 Department of Civil and Environmental Engineering, Incheon National University, Incheon 22012, Korea
6 Incheon Disaster Prevention Research Center, Incheon National University, Incheon 22012, Korea
* Correspondence: jongp24@incheon.ac.kr; Tel.: +82-32-835-8463

Received: 13 June 2017; Accepted: 18 July 2017; Published: 25 July 2017

Abstract: This paper investigates the effectiveness of four different soft computing methods, namely radial basis neural network (RBNN), adaptive neuro fuzzy inference system (ANFIS) with subtractive clustering (ANFIS-SC), ANFIS with fuzzy c-means clustering (ANFIS-FCM) and M5 model tree (M5Tree), for predicting the ultimate strength and strain of concrete cylinders confined with fiber-reinforced polymer (FRP) sheets. The models were compared according to the root mean square error (RMSE), mean absolute relative error (MARE) and determination coefficient (R^2) criteria. Similar accuracy was obtained by RBNN and ANFIS-FCM, and they provided better estimates in modeling ultimate strength of confined concrete. The ANFIS-SC, however, performed slightly better than the RBNN and ANFIS-FCM in estimating ultimate strain of confined concrete, and M5Tree provided the worst strength and strain estimates. Finally, the effects of strain ratio and the confinement stiffness ratio on strength and strain were investigated, and the confinement stiffness ratio was shown to be more effective.

Keywords: fiber reinforced polymer; concrete; column; confinement; stress; strain; model

1. Introduction

In recent years, the strengthening of existing concrete structures using externally bonded composite sheets of fiber reinforced polymer (FRP) has gained significant popularity. One common technique is wrapping unidirectional FRPs around the circumference of a concrete column to increase its axial strength and ductility. It is well-known that a concrete core expands laterally under uniaxial compression, but such expansion is confined by the FRP. Therefore, the core is subjected to a three-dimensional compressive state of stress in which the performance of the concrete core is significantly influenced by the confining pressure [1–5].

Many researchers studied the behavior of FRP-confined concrete and proposed a variety of confinement models for the ultimate condition of confined concrete under uniaxial compression loadings [6,7]. The majority of FRP confinement models are design-oriented and were developed using a regression analysis [8–12]. There have also been several analysis-oriented models developed based on the mechanics of confinement and strain compatibility between concrete and the FRP

wrap [13–15]. Recently, a new category of models has been proposed based on soft computing methods, such as artificial neural networks, generic algorithms, and fuzzy logic. Models in this category can handle complex databases containing a large number of independent variables, identify the sensitivity of input parameters, and provide mathematical solutions between dependent and independent variables [16]. Pham and Hadi [16] proposed the utilization of neural networks to compute the strain and compressive strength of FRP-confined columns, and the results show agreement between proposed neural network models and experimental data. Also, there are several studies related to design-oriented and analysis-oriented models [9,17–29].

Lim et al. [30] proposed a new model for evaluating the ultimate condition of FRP-confined concrete using genetic programming (GP). The model was the first to establish the ultimate axial strain and hoop rupture strain expressions for FRP-confined concrete on the basis of evolutionary algorithms. The results showed that the predictions from the suggested model aligned with a database compiled by the authors. The proposed models provided improved predictions compared to the existing artificial intelligence models. The model proved that more accurate results can be achieved in explaining and formulating the ultimate condition of FRP-confined concrete. The model assessment presented in that study clearly illustrated the importance of the size of the test databases and the selected test parameters used in the development of artificial intelligence models on their overall performance.

This paper studies the capability of four soft computing techniques for predicting the ultimate strength and strain of FRP-confined concrete cylindrical specimens. The computing techniques include radial basis neural network (RBNN), adaptive neuro fuzzy inference system (ANFIS) with subtractive clustering (ANFIS-SC), ANFIS with fuzzy c-means clustering (ANFIS-FCM), and M5 model tree (M5Tree).

2. Overview of Soft Computing Approaches

2.1. Radial Basis Function Neural Network

Artificial neural networks (ANNs) are inspired by biological neural networks. ANNs include a set of processing components, called neurons, which operate in parallel processes and transmit information to other neurons, similar to the functioning of a biological brain. ANNs are an efficient method for modeling complex input-output relationships and can learn relationships directly from the data being modeled [31]. The nonlinearity within a radial basis function (RBF) network can be selected from a few classic nonlinear functions. The hidden layer carries out a fixed nonlinear transformation with no adjustable variables, and it maps the input onto a new layer. The output layer then performs a linear combination on this new layer, and the only adjustable variables are the weights of this linear combiner [32]. A general RBF network is schematically illustrated in Figure 1.

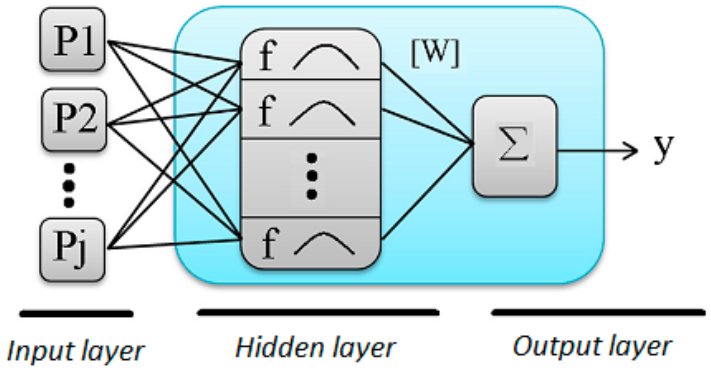

Figure 1. Schematic of a RBF network [31].

The radial basis function neural network (RBFN) model, which includes an input, an output and a single hidden layer, was developed by Powell [33] and Broomhead and Lowe [34]. In this model,

the number of input and output nodes is similar to that of multi-layer perceptron (MLP) neural networks, and was selected using the nature of real input and output parameters. However, the rate of learning in RBFN is much faster than the MLP method. The output of RBFN can be calculated with the following equation:

$$Y = \sum_{p=1}^{p} W_p \, \theta\left(\|X - X_p\|\right) \tag{1}$$

In the equation, W_p is the weight connecting the output nodes and hidden nodes, θ represents the radial basis function, X and Y are the input and output variables, X_P indicates the center of each hidden node which is dependent on the input data, and $\|X - X_p\|$ represents the Euclidean metric between hidden and input nodes. Each group of input nodes which has identical information as the input is indicated by one hidden node, and the transformation related to any node within the hidden layer is named a Gaussian function [35]. More detailed information about RBNN theory can be obtained from Haykin [36].

2.2. Adaptive Neuro Fuzzy Inference System

ANFIS is a combined intelligent system including ideas from neural networks and fuzzy control, combining the advantages of both. Fuzzy logic is a superset of typical logic that has been improved to operate with uncertain data and the theory of partial truth [37,38]. The most important disadvantage of fuzzy logic is the lack of a systematic approach to choosing membership function variables and designing the fuzzy rules. On the other hand, ANN has the ability to learn its structure from the input-output sets.

Jang [39] introduced ANFIS as a universal approximation which can estimate any real continued function on a compact data set with the desired precision [40,41]. In terms of function, ANFIS can be considered as equivalent to fuzzy inference systems, and the ANFIS system used can be considered as comparable to the Sugeno first-order fuzzy model [42]. A simple example is presented below, in which a fuzzy inference system was assumed with two inputs of x and y and one output of z. For this example, the typical rule set of a first-order Sugeno fuzzy model, which possess two simple fuzzy If-Then rules, is as follows:

$$\text{Rule 1}: \text{ IF x is A1, y is B1 and z is C1 THEN } f_1 = p_1 x + q_1 y + r_1 z + t_1 \tag{2}$$

$$\text{Rule 2}: \text{ IF x is A2, y is B2 and z is C2THEN } f_2 = p_2 x + q_2 y + r_2 z + t_2 \tag{3}$$

In the rule set, p_1, q_1, r_1 and p_2, q_2, r_2 are the variables of the THEN-part of the first-order Sugeno fuzzy model.

The ANFIS system uses a hybrid-learning algorithm to update parameters [43]. This algorithm is composed of two methods: the least squares approach and the gradient descent method. The function of the gradient descent approach is to adjust the variables of premise non-linear membership function, and the function of least squares method is to determine the resultant linear variables $\{p_i, q_i, r_i\}$. The learning process of this system has two steps. The first step includes the identification of consequent variables by the least squares method, while the prior variables are assumed to be fixed for the running cycle by the training set. After that, the error signals will spread backwards. In this part, the function of the gradient descent method includes updating the premise variables by minimizing the cost function, while the resultant variables stay fixed. Jang [39] presented the details of this algorithm and mathematical foundations of the hybrid learning algorithm.

In the present paper, two different ANFIS methods, including ANFIS with subtractive clustering (ANFIS-SC) and ANFIS with fuzzy c-means clustering (ANFIS-FCM),are utilized as modeling techniques. Subtractive clustering (SC) is an extension of the mountain clustering method suggested by Yager and Filev [44]. In this method, the data are clustered by evaluating the potential of data in the specification space. FCM is the modified K-means algorithm; it has some restrictions and may not

operate properly with large data sets. FCM minimizes within cluster variance and the classification of data using the clustering algorithm [45]. FCM works by minimizing the squared error function.

2.3. M5 Model Tree

Quinlan [46] explained the M5Tree, which includes a regression function at the terminal nodes. In fact, the M5 algorithm employs the idea of splitting the parameter space into subspaces and building a local linear regression model in each. The splitting follows the concept used in building a decision tree (see Figure 2).

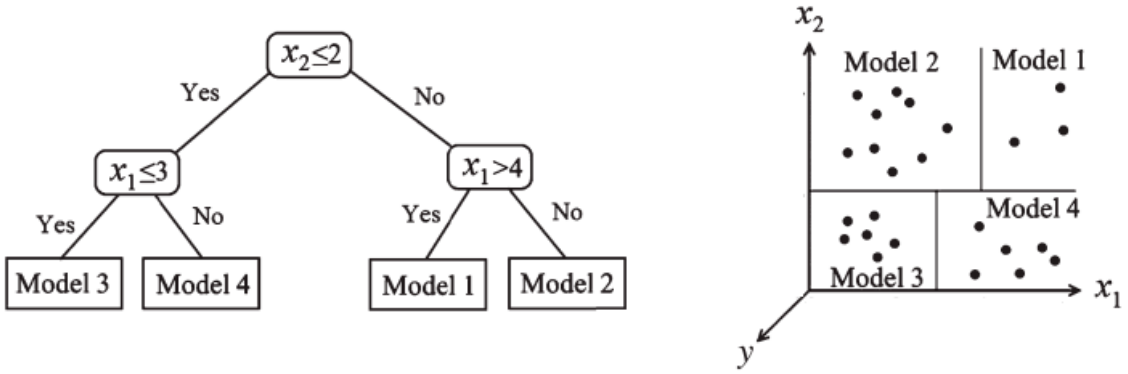

Figure 2. M5 tree; splitting the input space into subspaces and the resultant diagram [47].

The divide-and-conquer method is usually utilized to construct these types of tree-based models. Constructing a model tree entails two distinct steps. The first step includes a splitting criterion for the creation of a decision tree. In the M5Tree approach, this criterion is dependent on the standard deviation of the class values and then obtaining the decrement that can be expected in this error. The standard deviation reduction (SDR) can be calculated with the following equation:

$$SDR = sd(T) - \sum \frac{|T_i|}{T} sd(T_i) \quad (4)$$

In the equation, T indicates a set of instances that achieves the node, T_i is the subset of instances that have the ith result of the potential set, and sd is the standard deviation. The disarticulating proceeding causes the data in parent nodes to have more standard deviation compared to child nodes so that these data are purer. Once all the feasible splits are assessed, M5 selects the one that provides the maximum value for the expected error decrease. This grouping usually leads to a tree-like structure that should be trimmed by substituting a sub-tree, for example, with a leaf. In the next step, this tree growth must be trimmed and the sub-trees replaced with regression functions. In this method, the variable space is divided into several areas (subspaces), and a linear regression model is created for each of them. Quinlan [46] provides further details on M5Tree.

3. Results

In this study, four different soft computing techniques, i.e., RBNN, ANFIS-SC, ANFIS-FCM and M5 Tree, are employed for predicting strength (f'_{cc}/f'_{co}) and strain ($\varepsilon_{cc}/\varepsilon_{co}$). For the model simulations, a MATLAB neural network and fuzzy tool boxes are used, and 519 experimental data are adopted from Sadeghian and Fam [48,49]. Figure 3 shows the usual test setup for confined cylinders. Also, the statistical analyses of the input data employed in this study are summarized in Table 1. The data are used to develop models for ultimate strength and strain based on the strain ratio (ρ_ϵ) and the confinement stiffness ratio (ρ_K) inputs, which are defined as follows [48]:

$$f_l = \rho_K \rho_\varepsilon f'_{co} = \frac{2E_f \varepsilon_{h,rup} t}{D} \tag{5}$$

$$\rho_K = \frac{2E_f t}{(f'_{co}/\varepsilon_{co})D} \tag{6}$$

$$\rho_\varepsilon = \frac{\varepsilon_{h,rup}}{\varepsilon_{co}} \tag{7}$$

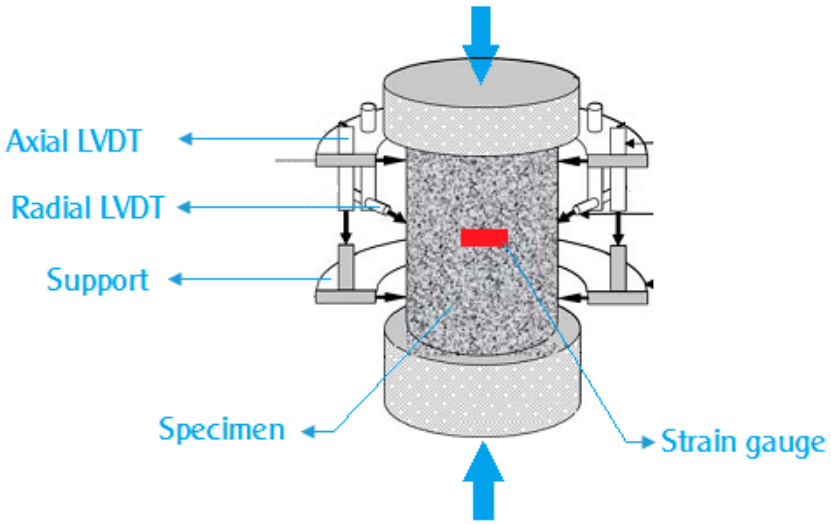

Figure 3. Test setup and instrumentation [50].

Table 1. Statistics for the experimental data.

	D (mm)	t (mm)	f'_{co} (MPa)	f'_{cc} (MPa)	ε_{co} (%)	ε_{cc} (%)	$\varepsilon_{h,rup}$ (%)	ρ_ε	E_f (GPa)	ρ_K
Min. value	51.00	0.09	19.70	31.40	0.20	0.23	0.10	0.29	10.50	0.01
Max. value	406.00	7.26	188.20	372.20	0.35	6.20	4.98	23.03	662.50	0.68
Average	158.46	0.89	46.52	83.88	0.24	1.68	1.12	4.80	183.09	0.07
Standard deviation	52.74	1.06	27.05	42.18	0.03	1.05	0.53	2.44	124.73	0.07

In the equations, f'_{co} is the unconfined concrete strength, ε_{co} is the corresponding axial strain of f'_{co}, E_f is the elastic modulus of the FRP wrap in the hoop direction, t is the total thickness of the FRP wrap, $\varepsilon_{h,rup}$ is the actual hoop rupture strain of the FRP wrap, and D is the diameter of the concrete core. The confinement ratio (f_l/f'_{co}) is a frequently used parameter in existing confinement models, which is equal to the product of ρ_K and ρ_ε. Several equations have been proposed for estimating the strain and strength of FRP-confined concrete cylinders which depend on ρ_K and ρ_ε [9,48]. According to Teng et al. [11], instead of the more approximate value of 0.002 for ε_{co}, it is assumed as follows:

$$\varepsilon_{co} = 9.37 \times 10^{-4} \sqrt[4]{f'_{co}}, \quad f'_{co} \, in \, MPa \tag{8}$$

The data set is randomly grouped into two subsets; the first data set is adopted for training, and the second data set (20% of the whole database) is adopted for the testing stage. Before application of the RBNN, the training values of input and output are normalized between 0.2 and 0.8 as follows:

$$b_1 \frac{x_i - x_{\min}}{x_{\max} - x_{\min}} + b_2 \tag{9}$$

In the equation, x_{max} and x_{min} are the maximum and minimum values of the training data. Here values of 0.6 and 0.2 are respectively assigned for b_1 and b_2, and the input data are normalized within a range of 0.2 to 0.8, as recommended in Cigizoglu [51]. According to that study, input parameters ranging from 0.2 to 0.8 allow the artificial neural network the flexibility to appraise beyond the training range.

The applied models are compared with the mean absolute relative error (MARE), root mean square error (RMSE) and determination coefficient (R^2). The definitions of statistical parameters are given as follows:

$$RMSE = \sqrt{\frac{1}{N}\sum_{i=1}^{N}(Xo_i - Xe_i)^2} \quad (10)$$

$$MARE = \frac{1}{N}\sum_{i=1}^{N}\frac{|Xo_i - Xe_i|}{Xo_i} \times 100 \quad (11)$$

where N, Xo_i and Xe_i are the number of samples, and the observed and estimated values, respectively.

3.1. Ultimate Strength Prediction

Testing and training results for the prediction of strength of the RBNN, ANFIS-SC, ANFIS-FCM and M5Tree models are listed in Table 2. The control parameter values of the optimal models are also provided in the second column. Different numbers of parameters and structures were tried for each method and the optimal ones were selected. Gaussian membership functions are used in ANFIS-SC and ANFIS-FCM models. The RBNN, ANFIS-SC and ANFIS-FCM methods can be easily obtained and applied by using new RBNN, genfis2 and genfis3 tools in MATLAB command windows. For the M5Tree method, code which is available for free online (http://www.cs.rtu.lv/jekabsons/regression.html) is used.

Table 2. Statistical performance of RBNN, ANFIS-SC, ANFIS-FCM and M5Tree models in strength predictions.

Method	Control Parameters	Training			Test		
		RMSE	MARE	R^2	RMSE	MARE	R^2
RBNN	0.8,15	0.32	11.6	0.880	0.27	10.5	0.899
ANFIS-SC	0.1	0.31	11.1	0.891	0.32	11.3	0.879
ANFIS-FCM	10	0.30	11.0	0.896	0.27	10.7	0.903
M5Tree		0.26	8.25	0.921	0.43	14.3	0.739

In the table, 0.8 and 15 indicate the spread value and the number of hidden layer neuron of the RBNN model, respectively, while 0.1 and 10 show the radii and cluster number of the ANFIS-SC and ANFIS-FCM models. A radii value of 0.1 in ANFIS-FCM corresponds to 15 clusters. This means that the ANFIS-FCM has fewer membership functions and parameters (10 Gaussian membership function each have 2 parameters, or 20 parameters in total) than those of ANFIS-SC. Table 2 implies that RBNN and ANFIS-FCM have almost the same accuracy, and they both are more efficient than the ANFIS-SC and M5Ttree models with respect to RMSE, MARE and R^2. It is interesting that the M5Tree approximated training data very well whereas its test results are worse than those of the other models. This implies that this method cannot adequately learn the investigated phenomenon. Different statistical indices were obtained for each of the methods. The main reason for this may be the fact that each method has different assumptions in developing models and their behaviors with the used data are distinct from each other. The rule base of the optimal ANFIS-FCM model is given in Table 3.

Table 3. Rule base of the optimal ANFIS-FCM in modeling strength.

1.	If (strain-ratio is in1cluster1) and (confinement-stiffness-ratio is in2cluster1) then (Strength is out1cluster1)
2.	If (strain-ratio is in1cluster2) and (confinement-stiffness-ratio is in2cluster2) then (Strength is out1cluster2)
3.	If (strain-ratio is in1cluster3) and (confinement-stiffness-ratio is in2cluster3) then (Strength is out1cluster3)
4.	If (strain-ratio is in1cluster4) and (confinement-stiffness-ratio is in2cluster4) then (Strength is out1cluster4)
5.	If (strain-ratio is in1cluster5) and (confinement-stiffness-ratio is in2cluster5) then (Strength is out1cluster5)
6.	If (strain-ratio is in1cluster6) and (confinement-stiffness-ratio is in2cluster6) then (Strength is out1cluster6)
7.	If (strain-ratio is in1cluster7) and (confinement-stiffness-ratio is in2cluster7) then (Strength is out1cluster7)
8.	If (strain-ratio is in1cluster8) and (confinement-stiffness-ratio is in2cluster8) then (Strength is out1cluster8)
9.	If (strain-ratio is in1cluster9) and (confinement-stiffness-ratio is in2cluster9) then (Strength is out1cluster9)
10.	If (strain-ratio is in1cluster10) and (confinement-stiffness-ratio is in2cluster10) then (Strength is out1cluster10)

Table 3 demonstrates that the model has 10 clusters and one rule for each of them. Figure 4 illustrates the strength estimates of the applied models in the forms of time variation and scatterplot.

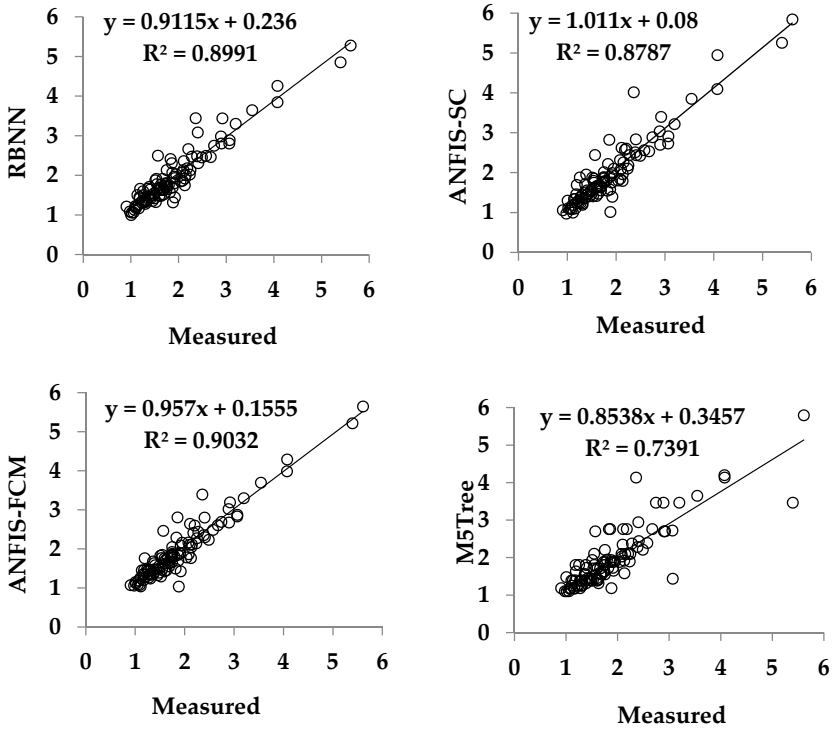

Figure 4. Strength estimates of the RBNN, ANFIS-SC, ANFIS-FCM and M5Tree models (dimensionless: f'_{cc}/f'_{co}).

From the figure, it is apparent that the RBNN and ANFIS-FCM models have less scattered assessments than other models, and the M5Tree model gave the most scattered estimates. This reveals that the investigated phenomenon is nonlinear, and therefore linear M5Tree cannot adequately simulate strength behavior. The variation of strength versus strain ratio and confinement stiffness ratio for the optimal ANFIS-FCM model is illustrated in Figure 5, in which it is clear that strength takes its maximum value when the strain ratio is also at its maximum.

The linear behavior for a confinement-stiffness-ratio greater than 0.3 is observed in Figure 5. This is because of the exponent of the confinement-stiffness-ratio in equations is usually 0.7; therefore, values greater than $0.3^{0.7}$ behave linearly.

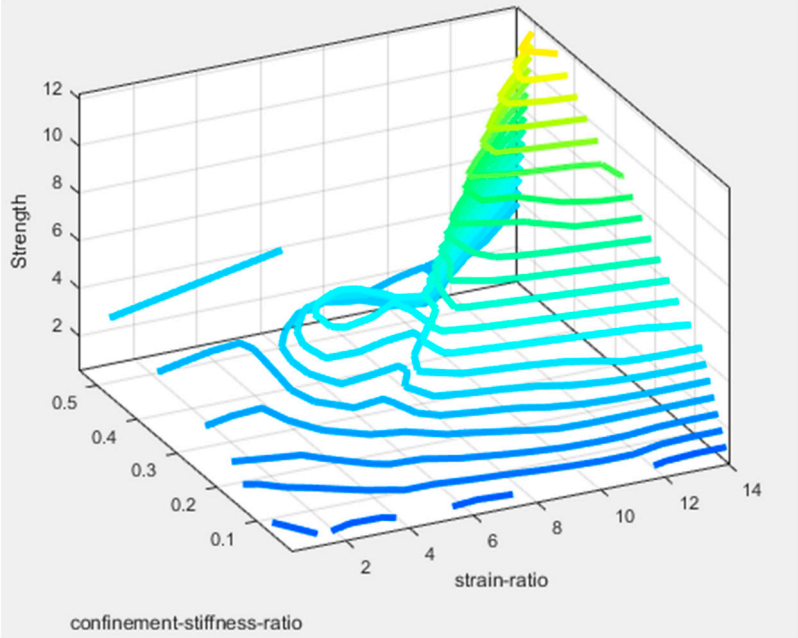

Figure 5. Variation of strength versus strain ratio and confinement stiffness ratio for the optimal ANFIS-FCM model.

3.2. Ultimate Strains Prediction

Strain predictions for the RMSE, MARE and R^2 values of the applied models are compared in Table 4.

Table 4. Statistical performance of RBNN, ANFIS-SC, ANFIS-FCM and M5Tree models in strain predictions.

Method	Control Parameters	Training			Test		
		RMSE	MARE	R^2	RMSE	MARE	R^2
RBNN	0.640	2.43	29.9	0.767	2.51	31.6	0.752
ANFIS-SC	0.1	2.31	29.4	0.790	2.47	30.5	0.766
ANFIS-FCM	6	2.33	31.3	0.786	2.57	31.9	0.742
M5Tree		1.90	21.8	0.858	2.72	33.3	0.711

This tables shows that the ANFIS-SC models outperform other models. Here also RBNN and ANFIS-FCM have similar accuracy, and they are slightly worse than the ANFIS-SC model. A radii value of 0.1 in ANFIS-SC corresponds to 13 clusters. Similar to the previous application, here too ANFIS-SC has many more membership functions and parameters compared to ANFIS-FCM. Table 5 gives the rule base of the optimal ANFIS-SC model. The estimated results of the optimal RBNN, ANFIS-FCM and ANFIS-SC models are shown in Figure 6.

This figure shows that the estimates of the ANFIS-SC model are closer to the corresponding measured values, especially for high strain values. The variation of strength versus strain ratio and confinement stiffness ratio for the optimal ANFIS-SC model is shown in Figure 7. It is clear from the figure that strain takes its maximum value when the strain ratio and confinement stiffness ratio are both at their maximum values. The linear relationship between strain and strain ratio is clearly seen in the range of confinement-stiffness-ratio between 0.4 and 0.6.

The effects of strain ratio and the confinement stiffness ratio inputs on strength and strain were also investigated using the ANFIS-SC method because it has less control parameters than RBNN. For the RBNN models, the optimal radii and hidden node numbers should be determined

whereas, in obtaining ANFIS-SC model, the radii value which indicates the number of clusters is only distinguished. The simulation results of the ANFIS-SC models are reported in Table 6.

Table 5. Rule base of the optimal ANFIS-SC in modeling strain.

1.	If (strain-ratio is in1cluster1) and (confinement-stiffness-ratio is in2cluster1) then (Strength is out1cluster1)
2.	If (strain-ratio is in1cluster2) and (confinement-stiffness-ratio is in2cluster2) then (Strength is out1cluster2)
3.	If (strain-ratio is in1cluster3) and (confinement-stiffness-ratio is in2cluster3) then (Strength is out1cluster3)
4.	If (strain-ratio is in1cluster4) and (confinement-stiffness-ratio is in2cluster4) then (Strength is out1cluster4)
5.	If (strain-ratio is in1cluster5) and (confinement-stiffness-ratio is in2cluster5) then (Strength is out1cluster5)
6.	If (strain-ratio is in1cluster6) and (confinement-stiffness-ratio is in2cluster6) then (Strength is out1cluster6)
7.	If (strain-ratio is in1cluster7) and (confinement-stiffness-ratio is in2cluster7) then (Strength is out1cluster7)
8.	If (strain-ratio is in1cluster8) and (confinement-stiffness-ratio is in2cluster8) then (Strength is out1cluster8)
9.	If (strain-ratio is in1cluster9) and (confinement-stiffness-ratio is in2cluster9) then (Strength is out1cluster9)
10.	If (strain-ratio is in1cluster10) and (confinement-stiffness-ratio is in2cluster10) then (Strength is out1cluster10)
11.	If (strain-ratio is in1cluster11) and (confinement-stiffness-ratio is in2cluster11) then (Strength is out1cluster11)
12.	If (strain-ratio is in1cluster12) and (confinement-stiffness-ratio is in2cluster12) then (Strength is out1cluster12)
13.	If (strain-ratio is in1cluster13) and (confinement-stiffness-ratio is in2cluster13) then (Strength is out1cluster13)

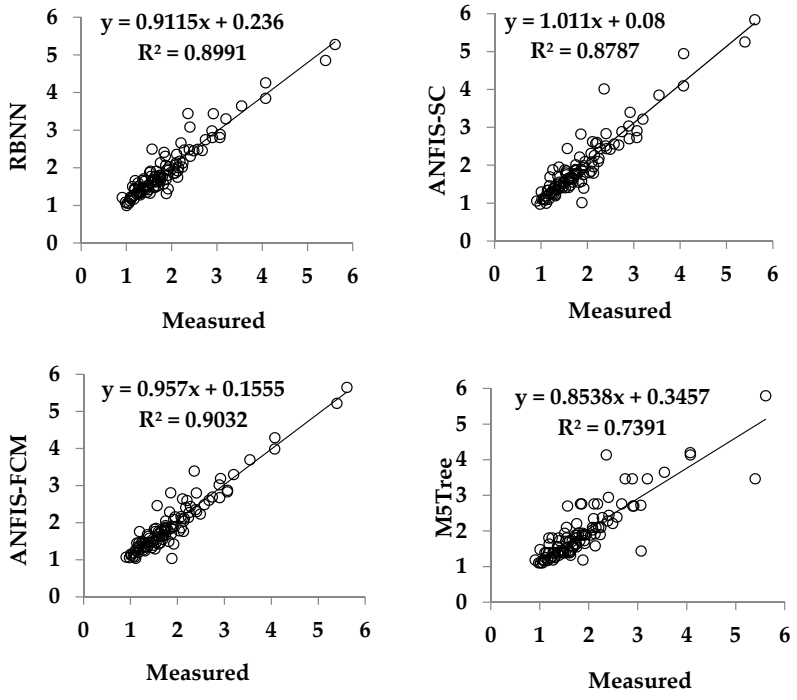

Figure 6. Strain estimates of the RBNN, ANFIS-SC, ANFIS-FCM and M5Tree models (dimensionless: $\varepsilon_{cc}/\varepsilon_{co}$).

Table 6. Effect of strain ratio (ρ_ϵ) and the confinement stiffness ratio (ρ_K) inputs on strength and strain with respect to ANFIS-SC.

Inputs	Control Parameters	Training			Test		
		RMSE	MARE	R^2	RMSE	MARE	R^2
				Strength			
ρ_ϵ	0.1	0.852	32.8	0.249	0.804	32.8	0.054
ρ_K	0.1	0.646	21.3	0.512	0.648	25.1	0.445
				Strain			
ρ_ϵ	0.2	4.081	63.6	0.343	4.406	59.2	0.244
ρ_K	0.1	4.453	71.8	0.218	4.330	63.2	0.265

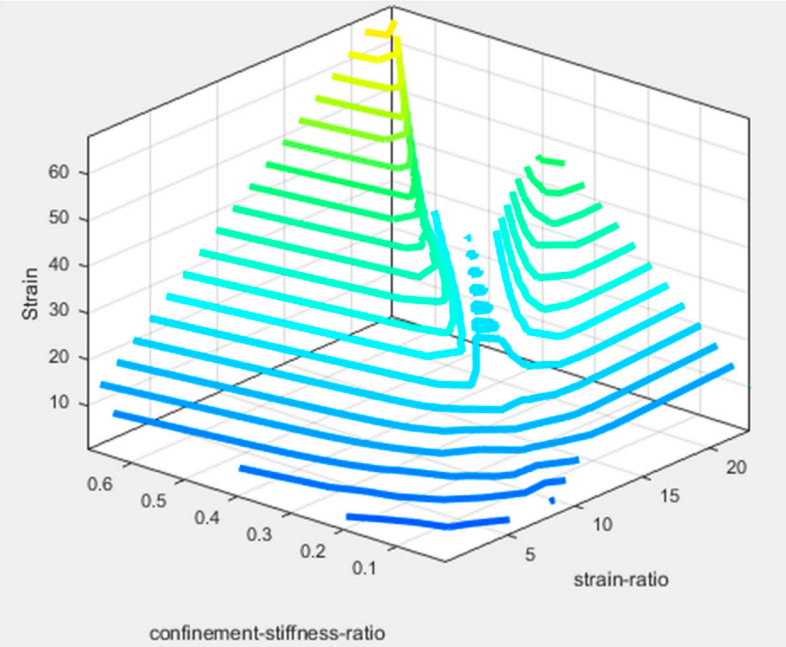

Figure 7. Variation of strain versus strain ratio and confinement stiffness ratio for the optimal ANFIS-SC model.

This table indicates that the effect of ρ_K is more significant than ρ_ϵ in strength and strain. The relative RMSE differences between ρ_K and ρ_ϵ based ANFIS-SC models are 19.4% and 1.7% for strength and strain, respectively.

It should be noted that providing explicit formulation for the RBNN, ANFIS-SC and ANFIS-FCM is impossible because they are black-box models. However, the regression tree of the optimal M5Tree models for the strain and strength modeling are provided in Appendix A.

4. Conclusions

In this paper, the ultimate strength and strain of cylindrical concrete specimens confined with FRP composites were studied using four soft computational methods. The optimal RBNN, ANFIS-SC, ANFIS-FCM and M5Tree models obtained by trying different control parameters were compared with respect to RMSE, MARE and R^2 statistics. RBNN and ANFIS-FCM provided almost the same level of accuracy, and they performed better than the other models in estimating strength of FRP-confined concrete cylindrical specimens by using the inputs of strain ratio and the confinement stiffness ratio. In estimating strain of FRPs, however, the ANFIS-SC model performed slightly better than the RBNN and ANFIS-FCM models. Among the applied models, the M5Tree model was the least accurate at estimating strength and strain of FRPs. The effects of strain ratio and the confinement stiffness ratio inputs on strength and strain were also examined using ANFIS-SC, and the confinement stiffness ratio was found to be more significant than strain ratio in strength and strain.

Acknowledgments: This research was supported by the Basic Science Research Program through the National Research Foundation of Korea (NRF), which is funded by the Ministry of Science, ICT & Future Planning of the Republic of Korea (2017R1A2B2010120).

Author Contributions: Pedram Sadeghian conceived and designed the database; Ozgur Kisi and Iman Mansouri analyzed the data; Jong Wan Hu and Iman Mansouri wrote the paper. Chang-Hwan Lee also analyzed the data and handled the final proofreading.

Conflicts of Interest: The authors declare no conflict of interest.

Appendix A. Regression Tree of the Optimal M5Tree Models for the Strain and Strength Modeling

Table A1. Regression tree obtained from M5Tree for strength modeling.

```
if x2 <= 0.065174

if x2 <= 0.0255
   if x1 <= 2.9025
    if x1 <= 2.505
      y = 1.108064681 (10)
    else
      y = 0.891721241833333 (6)
   else if x2 <= 0.021267
      if x2 <= 0.010372

       y = 1.483590448 (4)
      else if x2 <= 0.015328
         y = 1.13560753725 (12)
       else if x2 <= 0.018965
          y = 1.25916023821429 (14)
         else
         y = 1.1897478106 (5)
      else if x1 <= 6.5213
       if x1 <= 4.9928
         y = 1.26759138458333 (12)
       else
         y = 1.3995581252 (5)

      else if x1 <= 7.387

         y = 1.654221567 (4)
       else


         y = 1.4358405485 (4)

else if x1 <= 7.0025
    if x1 <= 3.4344
      if x2 <= 0.029531
       y = 1.16075967033333 (6)
      else if x1 <= 1.3994
         y = 1.179568198 (4)
       else if x2 <= 0.059018
          y = 1.39728594933333 (24)
         else
          y = 1.59811338542857 (7)
    else if x2 <= 0.04595
      if x2 <= 0.033094
        if x1 <= 5.5058
         y = 1.323997823 (12)
         else


         y = 1.56201983057143 (7)
        else if x2 <= 0.034551
          if x2 <= 0.033937

             y = 1.71921529875 (4)
           else
             y = 1.92418515966667 (6)
           else if x2 <= 0.037414
             y = 1.45295335707692 (13)
           else if x2 <= 0.044137
             y = 1.73181401571429 (14)

           else if x2 <= 0.045434
               y = 1.41987727225 (4)
             else
               y = 1.587916394 (4)
         else if x1 <= 3.7759
           y = 1.64059121775 (4)
         else if x2 <= 0.056561
           if x2 <= 0.04728
             y = 1.7582115855 (4)
           else if x2 <= 0.050345
             y = 2.23252585925 (4)
           else


             y = -4.7981786875333
+124.346272222065*x2 (9)
           else
           y = 2.72437967584461 −
0.199395562322418*x1 (13)
      else if x2 <= 0.049162
        if x2 <= 0.037766

         if x1 <= 8.8613
           if x2 <= 0.033956
           y = 1.7132418315 (12)
           else
           y = 1.89220380857143 (7)
         else
           y = 2.15360432216667 (6)
        else
         y = 2.21282843818182 (11)
      else if x1 <= 7.8378
        y = 2.3919454476 (5)
       else
        y = 2.915657196 (7)
else if x1 <= 6.6355
   if x2 <= 0.15871

    if x1 <= 3.3762
      if x2 <= 0.071835
       y = 1.55785802183333 (6)
      else if x1 <= 2.6111
         y = 1.8102727921 (20)
       else
         y = 1.57794946244278
+4.99230783389806*x2 (11)
    else if x2 <= 0.092595
      if x2 <= 0.06805
        if x2 <= 0.066642
         y = 2.34944086616667 (6)
        else
         y = 2.7420408164 (5)
      else if x2 <= 0.074024
         y = 1.9024165688 (5)
        else
         y = 2.10530567306667 (15)
else if x1 <= 3.9987
        y = 5.07504348861174
-23.5904126567999*x2 (11)
      else if x2 <= 0.10281

         y = 2.9481859308 (5)
        else

         y = 2.70621362185714 (7)
   else if x1 <= 2.9764

      y = 2.767153359 (19)
    else if x2 <= 0.22102
      y = 3.47170636066667 (9)
     else
      y = 4.1398758346 (5)
else if x2 <= 0.13591
   if x2 <= 0.068264
     y = 2.72699884416667 (6)
   else if x2 <= 0.1031
     y = 3.65529982828571 (7)
    else
     y = 4.204802991 (4)
  else
    y = 1.45436334578442
+23.9129270980071*x2 (10)
```

Table A2. Regression tree obtained from M5Tree for strain modeling.

```
if x1 <= 6.2548

if x2 <= 0.06311
   if x1 <= 3.6413
    if x2 <= 0.020455

      if x1 <= 1.8874
       y = 1.1440491595 (6)
      else
       y = 1.68687631466667 (9)
    else if x1 <= 2.6807

      if x1 <= 2.2516
        if x1 <= 1.7107
         y = 1.78844272172727 (11)

        else
         y = 3.15371412385714 (7)
      else
        y = 1.764552396 (6)
    else if x2 <= 0.047075

        if x2 <= 0.035327
         if x1 <= 3.4003
           y = 2.8827251381 (10)
         else
           y = 4.1709103866 (5)
        else

         y = 3.072717053875 (8)

      else
        y = 4.18276414975 (12)
   else if x2 <= 0.021073
     if x2 <= 0.018742
      y = 2.46492040855556 (9)
     else
      y = 3.35411568575 (4)
  else if x1 <= 4.0509
     if x2 <= 0.054126
       y = 4.0987042836 (15)
     else
       y = 6.1883060684 (5)

    else if x2 <= 0.033258
       if x1 <= 5.6609
        if x2 <= 0.024021
          y = 6.21866667766667 (6)
        else if x2 <= 0.029178
          y = 2.6673381094 (5)
           else
            y = 4.69127474228571 (7)

         else
          y = 6.3533113762 (5)

      else if x1 <= 5.6305
        if x1 <= 4.5915
          if x2 <= 0.038697
           y = 5.82153494575 (4)
          else if x2 <= 0.055755

            y = 7.6093721018 (5)
          else
            y = 6.4901269452 (5)

        else
          y = 6.42120672495833 (24)
        else
         y = 8.64814412742857 (7)

else if x1 <= 2.8545
   if x2 <= 0.14161
     if x1 <= 0.94068
      y = 1.6541689808 (5)
     else if x2 <= 0.12452
       if x2 <= 0.091846
        y = 3.8282330848 (10)

       else

        y = 5.62676665785714 (7)
      else
        y = 3.269071034 (4)
   else
     y = 7.55286884866667 (21)
  else if x2 <= 0.14818
     if x2 <= 0.092595
      if x1 <= 4.2573
        if x1 <= 3.429
         y = 7.9752687216 (5)
        else
         y = 10.9299345495055
-67.7789156702637*x2 (13)
       else if x1 <= 5.2858
        if x1 <= 4.3562
          y = 7.779023415 (4)
        else
          y = 9.292927947 (10)
           else
            y = 6.0040160536 (5)

    else if x2 <= 0.20919
       y = 2.39097472537744
+2.19876304626978*x1 (10)
      else
       y = 14.51223043 (8)
 else if x2 <= 0.05346
    if x2 <= 0.022672
     y = 3.41272976260672
+0.218464713423608*x1 (22)
    else if x1 <= 8.8613
      if x2 <= 0.033956
       y = 11.8427843384812
-146.164747121597*x2 (20)
      else if x2 <= 0.035225
        y = 12.096092072 (5)
       else if x2 <= 0.041997
         if x1 <= 7.2822
           y = 5.2413583345 (4)

         else
           y = 8.69478460875 (4)
        else
         y = 10.7816929114 (10)
    else
      y = −4.15948380355076
+1.79907971888928*x1 (8)

 else if x2 <= 0.14656
    if x1 <= 7.7892
      if x2 <= 0.067874
       y = 11.774363725 (6)
      else
       y = 15.9303924215 (8)
    else
      y = 17.838992625 (18)
   else
   y = 24.3989610371429 (7)
     else if x2 <= 0.11185
       y = 10.2661860479091 (11)
      else if x1 <= 4.1077

        y = 6.97833482855556 (9)
        else
        y = 9.9430306388 (5)
```

References

1. Green, M.F.; Bisby, L.A.; Fam, A.Z.; Kodur, V.K.R. Frp confined concrete columns: Behaviour under extreme conditions. *Cem. Concr. Compos.* **2006**, *28*, 928–937. [CrossRef]
2. Mirmiran, A.; Shahawy, M.; Samaan, M.; El Echary, H.; Mastrapa, J.C.; Pico, O. Effect of column parameters on frp-confined concrete. *J. Compos. Constr.* **1998**, *2*, 175–185. [CrossRef]
3. Nanni, A.; Bradford, N.M. Frp jacketed concrete under uniaxial compression. *Constr. Build. Mater.* **1995**, *9*, 115–124. [CrossRef]
4. Pessiki, S.; Harries, K.A.; Kestner, J.T.; Sause, R.; Ricles, J.M. Axial behavior of reinforced concrete columns confined with frp jackets. *J. Compos. Constr.* **2001**, *5*, 237–245. [CrossRef]
5. Sadeghian, P.; Rahai, A.R.; Ehsani, M.R. Effect of fiber orientation on compressive behavior of cfrp-confined concrete columns. *J. Reinf. Plast. Compos.* **2010**, *29*, 1335–1346. [CrossRef]

6. Mansouri, I.; Gholampour, A.; Kisi, O.; Ozbakkaloglu, T. Evaluation of peak and residual conditions of actively confined concrete using neuro-fuzzy and neural computing techniques. *Neural Comput. Appl.* **2016**, 1–16. [CrossRef]
7. Mansouri, I.; Ozbakkaloglu, T.; Kisi, O.; Xie, T. Predicting behavior of frp-confined concrete using neuro fuzzy, neural network, multivariate adaptive regression splines and m5 model tree techniques. *Mater. Struct. Materiaux Constr.* **2016**, *49*, 4319–4334. [CrossRef]
8. Karbhari, V.M.; Gao, Y. Composite jacketed concrete under uniaxial compression—Verification of simple design equations. *J. Mater. Civ. Eng.* **1997**, *9*, 185–193. [CrossRef]
9. Lam, L.; Teng, J.G. Design-oriented stress-strain model for frp-confined concrete. *Constr. Build. Mater.* **2003**, *17*, 471–489. [CrossRef]
10. Samaan, M.; Mirmiran, A.; Shahawy, M. Model of concrete confined by fiber composites. *J. Struct. Eng.* **1998**, *124*, 1025–1031. [CrossRef]
11. Teng, J.G.; Jiang, T.; Lam, L.; Luo, Y.Z. Refinement of a design-oriented stress-strain model for frp-confined concrete. *J. Compos. Constr.* **2009**, *13*, 269–278. [CrossRef]
12. Toutanji, H.A. Stress-strain characteristics of concrete columns externally confined with advanced fiber composite sheets. *ACI Mater. J.* **1999**, *96*, 397–404.
13. Harries, K.A.; Kharel, G. Behavior and modeling of concrete subject to variable confining pressure. *ACI Mater. J.* **2002**, *99*, 180–189.
14. Spoelstra, M.R.; Monti, G. Frp-confined concrete model. *J. Compos. Constr.* **1999**, *3*, 143–150. [CrossRef]
15. Fam, A.Z.; Rizkalla, S.H. Confinement model for axially loaded concrete confined by circular fiber-reinforced polymer tubes. *ACI Struct. J.* **2001**, *98*, 451–461.
16. Pham, T.M.; Hadi, M.N.S. Predicting stress and strain of frp-confined square/rectangular columns using artificial neural networks. *J. Compos. Constr.* **2014**, *18*, 1–9. [CrossRef]
17. Berthet, J.F.; Ferrier, E.; Hamelin, P. Compressive behavior of concrete externally confined by composite jackets: Part b: Modeling. *Constr. Build. Mater.* **2006**, *20*, 338–347. [CrossRef]
18. Bisby, L.A.; Dent, A.J.S.; Green, M.F. Comparison of confinement models for fiber-reinforced polymer-wrapped concrete. *ACI Struct. J.* **2005**, *102*, 62–72.
19. Cascardi, A.; Micelli, F.; Aiello, M.A. Unified model for hollow columns externally confined by frp. *Eng. Struct.* **2016**, *111*, 119–130. [CrossRef]
20. Cascardi, A.; Micelli, F.; Aiello, M.A. An artificial neural networks model for the prediction of the compressive strength of frp-confined concrete circular columns. *Eng. Struct.* **2017**, *140*, 199–208. [CrossRef]
21. Faustino, P.; Chastre, C. Analysis of load–strain models for rc square columns confined with cfrp. *Compos. Part B Eng.* **2015**, *74*, 23–41. [CrossRef]
22. Ilki, A.; Kumbasar, N.; Koc, V. Low strength concrete members externally confined with frp sheets. *Struct. Eng. Mech.* **2004**, *18*, 167–194. [CrossRef]
23. Matthys, S.; Toutanji, H.; Audenaert, K.; Taerwe, L. Axial load behavior of large-scale columns confined with fiber-reinforced polymer composites. *ACI Struct. J.* **2005**, *102*, 258–267.
24. Naderpour, H.; Kheyroddin, A.; Amiri, G.G. Prediction of frp-confined compressive strength of concrete using artificial neural networks. *Compos. Struct.* **2010**, *92*, 2817–2829. [CrossRef]
25. Rousakis, T.C.; Tourtouras, I.S. Modeling of passive and active external confinement of rc columns with elastic material. *ZAMM J. Appl. Math. Mech.* **2015**, *95*, 1046–1057. [CrossRef]
26. Saiidi, M.S.; Kandasamy, S.; Claudia, P. Simple carbon-fiber-reinforced-plastic-confined concrete model for moment-curvature analysis. *J. Compos. Constr.* **2005**, *9*, 101–104. [CrossRef]
27. Sidney, A.G.; Lukito, G. Strengthening of reinforced concrete bridge columns with frp wrap. *Pract. Period. Struct. Des. Constr.* **2006**, *11*, 218–228.
28. Tamuzs, V.; Tepfers, R.; Sparnins, E. Behavior of concrete cylinders confined by carbon composite 2. Prediction of strength. *Mech. Compos. Mater.* **2006**, *42*, 109–118. [CrossRef]
29. Teng, J.G.; Lin, G.; Yu, T. Analysis-oriented stress-strain model for concrete under combined frp-steel confinement. *J. Compos. Constr.* **2015**, *19*. [CrossRef]
30. Lim, J.C.; Karakus, M.; Ozbakkaloglu, T. Evaluation of ultimate conditions of frp-confined concrete columns using genetic programming. *Comput. Struct.* **2016**, *162*, 28–37. [CrossRef]
31. Zounemat-kermani, M.; Kisi, O.; Rajaee, T. Performance of radial basis and lm-feed forward artificial neural networks for predicting daily watershed runoff. *Appl. Soft Comput.* **2013**, *13*, 4633–4644. [CrossRef]

32. Senthil Kumar, A.R.; Ojha, C.S.P.; Goyal, M.K.; Singh, R.D.; Swamee, P.K. Modeling of suspended sediment concentration at kasol in india using ann, fuzzy logic, and decision tree algorithms. *J. Hydrol. Eng.* **2012**, *17*, 394–404. [CrossRef]
33. Powell, M.J.D. Radial basis functions for multivariable interpolation: A review. In Proceedings of the IMA Conference on Algorithms for the Approximation of Functions and Data, RMCS, Shrivenham, UK, 1–30 July 1987; pp. 143–167.
34. Broomhead, D.S.; Lowe, D. Multivariable functional interpolation and adaptive networks. *Complex Syst.* **1988**, *2*, 321–355.
35. Rezaeian-Zadeh, M.; Zand-Parsa, S.; Abghari, H.; Zolghadr, M.; Singh, V.P. Hourly air temperature driven using multi-layer perceptron and radial basis function networks in arid and semi-arid regions. *Theor. Appl. Climatol.* **2012**, *109*, 519–528. [CrossRef]
36. Haykin, S. *Neural Networks and Learning Machines*, 3rd ed.; Prentice Hall: New Jersey, NJ, USA, 2008.
37. Deka, P.; Chandramouli, V. Fuzzy neural network model for hydrologic flow routing. *J. Hydrol. Eng.* **2005**, *10*, 302–314. [CrossRef]
38. Yilmaz, A.G.; Muttil, N. Runoff estimation by machine learning methods and application to the euphrates basin in Turkey. *J. Hydrol. Eng.* **2014**, *19*, 1015–1025. [CrossRef]
39. Jang, J.S.R. Anfis: Adaptive-network-based fuzzy inference system. *IEEE Transact. Syst. Man Cybern.* **1993**, *23*, 665–685. [CrossRef]
40. Jang, J.S.R.; Sun, C.T.; Mizutani, E. *Neuro-Fuzzy and Soft Computing: A Computational Approach to Learning and Machine Intelligence*; Prentice-Hall Upper Saddle River: New Jersey, NY, USA, 1997.
41. Mansouri, I.; Kisi, O. Prediction of debonding strength for masonry elements retrofitted with frp composites using neuro fuzzy and neural network approaches. *Compos. Part B Eng.* **2015**, *70*, 247–255. [CrossRef]
42. Drake, J.T. Communications Phase Synchronization Using the Adaptive Network Fuzzy Inference System. Ph.D. Thesis, New Mexico State University, Albuquerque, NM, USA, 2000.
43. Mansouri, I.; Shariati, M.; Safa, M.; Ibrahim, Z.; Tahir, M.M.; Petković, D. Analysis of influential factors for predicting the shear strength of a v-shaped angle shear connector in composite beams using an adaptive neuro-fuzzy technique. *J. Intell. Manuf.* **2017**, *28*, 1–11. [CrossRef]
44. Yager, R.R.; Filev, D.P. Approximate clustering via the mountain method. *IEEE Transact. Syst. Man Cybern.* **1994**, *24*, 1279–1284. [CrossRef]
45. Ayvaz, M.T.; Karahan, H.; Aral, M.M. Aquifer parameter and zone structure estimation using kernel-based fuzzy c-means clustering and genetic algorithm. *J. Hydrol.* **2007**, *343*, 240–253. [CrossRef]
46. Quinlan, J.R. Learning with continuous classes. In Proceedings of the 5th Australian Joint Conference on Artificial Intelligence (AI '92), Hobart, Australia, 16–18 October 1992; Adams, A., Sterling, L., Eds.; World Scientific Publishing: Singapore, 1992; pp. 343–348.
47. Wang, L.; Kisi, O.; Zounemat-Kermani, M.; Zhu, Z.; Gong, W.; Niu, Z.; Liu, H.; Liu, Z. Prediction of solar radiation in China using different adaptive neuro-fuzzy methods and m5 model tree. *Int. J. Climatol.* **2017**, *37*, 1141–1155. [CrossRef]
48. Sadeghian, P.; Fam, A. Improved design-oriented confinement models for frp-wrapped concrete cylinders based on statistical analyses. *Eng. Struct.* **2015**, *87*, 162–182. [CrossRef]
49. Sadeghian, P.; Fam, A. A rational approach toward strain efficiency factor of fiber-reinforced polymer-wrapped concrete columns. *ACI Struct. J.* **2014**, *111*, 135–144.
50. Berthet, J.F.; Ferrier, E.; Hamelin, P. Compressive behavior of concrete externally confined by composite jackets. Part a: Experimental study. *Constr. Build. Mater.* **2005**, *19*, 223–232. [CrossRef]
51. Cigizoglu, H.K. Estimation, forecasting and extrapolation of river flows by artificial neural networks. *Hydrol. Sci. J.* **2003**, *48*, 349–362. [CrossRef]